IEEE Access
Multidisciplinary | Rapid Review | Open Access Journal

Received March 11, 2020, accepted March 29, 2020, date of publication April 1, 2020, date of current version April 17, 2020.

Digital Object Identifier 10.1109/ACCESS.2020.2984776

Predicting Trial-By-Trial Variation in Oculomotor Behavior Using Multivariate Electroencephalography Theta Phase

WOOJAE JEONG[1,2], SEOLMIN KIM[1,2], YEE-JOON KIM[3], AND JOONYEOL LEE[1,2], (Member, IEEE)

[1]Center for Neuroscience Imaging Research, Institute for Basic Science (IBS), Suwon 16419, South Korea
[2]Department of Biomedical Engineering, Sungkyunkwan University, Suwon 16419, South Korea
[3]Center for Cognition and Sociality, Institute for Basic Science (IBS), Daejeon 34126, South Korea

Corresponding author: Joonyeol Lee (joonyeol@g.skku.edu)

This work was supported by the Institute for Basic Science, South Korea, under Grant IBS-R015-D1. The work of Yee-Joon Kim was supported by the Institute for Basic Science, South Korea, under Grant IBS-R001-D1.

ABSTRACT When we interact with our environment, there is often a significant amount of variations in our behavioral responses to incoming sensory input even when inputs are identical. Variations in sensory-motor behavior can be caused by several factors, including changes in cognitive status and intrinsic neural variations in the brain. The correct identification of neural sources of behavioral variations is important for understanding the underlying neural mechanisms of sensory-motor behavior and for practical applications (e.g., the development of a precise brain-computer interface). However, studies on humans that investigate the neural sources of the trial-by-trial variation of the sensory-motor behavior are scarce. In this study, we explored the neural correlates of behavioral variations in smooth pursuit eye movements. We collected electroencephalography (EEG) activity from 15 participants while they performed a smooth pursuit eye movement task, wherein they tracked randomly selected visual motion targets that moved radially from the center of the screen. We isolated neural components that are specific to the trial-by-trial variation of smooth pursuit latency, speed, and direction using a novel multivariate pattern-analysis technique. We found that the phase of the spatially distributed multivariate theta oscillation was correlated with the trial-by-trial variation of pursuit latency and direction. This suggests that the changing patterns of the theta phase across EEG sensors can predict upcoming behavioral variations.

INDEX TERMS Brain computer interfaces, cognition, cognitive science, correlation, electroencephalography, machine learning, multivariate pattern-analysis.

I. INTRODUCTION

In information processing, our brain must tackle random unwanted noise that originates either from the external environment or from within the brain. We exhibit variable motor behaviors even when the same sensory inputs are encountered. This occurs in the simplest form of sensory-motor responses, irrespective of strong intentions to reproduce the same actions [1]. Some behavioral variations originate from neural variations inside the brain. Identifying the source of this neural noise is key to understanding trial-by-trial behavioral variations in movements [2]–[4]. The smooth pursuit eye movement, one of the three voluntary eye movements (saccades, smooth pursuit, and vergence) of human and non-human primates, is a simple sensory-guided oculomotor behavior triggered by visual motion. Previous studies conducted using rhesus monkeys reported that the correlated neural variations in the middle temporal visual area (area MT, which is an important area for processing sensory motion [5]–[8] and has a causal relationship with the initiation of smooth pursuit [9]), can partially account for trial-by-trial variations in smooth pursuit speed [10], direction [11], and latency [12]. The frontal eye field smooth eye movement region (FEF_{SEM}),

The associate editor coordinating the review of this manuscript and approving it for publication was Qichun Zhang.

which is important for controlling the gain of smooth pursuit eye movements [13], [14], is known to be involved in the trial-by-trial variations of smooth-pursuit latency; the correlated neural variations in this area can partially explain the latency variations [15]. Subcortical areas including the cerebellum [12], [16] and brain stem [12], [17] are also known to be important for the variation of smooth pursuit initiation, but those variations are inherited from the neural variation in cortical areas [10]–[12], [16]–[18].

In humans, the electroencephalography (EEG) imaging technique is suitable for studying the neural source of behavioral variations because 1) EEG activity would reflect the brain-wide cortical neural activity, and 2) of its superior temporal resolution (to functional magnetic resonance imaging techniques, for example). Furthermore, EEG has been widely used to develop a brain-computer interface [19], [20], thus the identification of neural sources of behavioral variations in EEG can contribute to the improvement of this system. Although there is an increasing need to investigate neural sources of trial-by-trial behavioral variations, studies based on the same on humans are scarce partly because the EEG signal is complex. EEG activity variations can derive from multiple sources, some of which are the true sources of specific behavioral variations, while others result from variation in the global internal states of the brain [21]. Besides, there may be other unexpected and uncontrolled sources, i.e. muscle activation-induced artifacts, cardiac artifacts or movement artifacts. Therefore, it is important to isolate the EEG activity variations that are specific to the variations in the behavior of interest. However, it is difficult to do so using traditional univariate approaches.

In this study, to isolate the EEG activity component specific to the variation of oculomotor behavioral modes (pursuit speed, latency, and direction), we directly estimated behavioral variations from the spatially distributed multivariate EEG activity patterns and searched for the EEG oscillation components that exhibited a meaningful trial-by-trial relationship with behavioral variations. We found that only the phase of theta oscillation (4–8 Hz) could predict variations in the latency and direction of oculomotor behavior.

II. METHODS

We collected EEG and behavioral data from 21 human participants with normal or corrected-to-normal vision. We discarded the data of six participants with poor pursuit eye movements and noisy EEG data. Among them, five were excluded because more than 30% of their trials had too-early saccadic eye movements, and one was excluded because more than 50% of the independent components (ICs) were rejected by the artifact rejection procedure (see Section II D). The data of the remaining 15 participants were analyzed and are presented in this paper (three females; 12 males; age range: 21–32 years). A portion of the data used has been published in a study in which an unrelated aspect was observed and analyzed [22]. All participants gave informed consent, and experimental procedures and methods were approved by the Institutional Review Board at Sungkyunkwan University.

A. STIMULI AND TASK DESIGN

Visual stimuli were displayed on a gamma-corrected 20-inch CRT monitor (Hewlett Packard P1230, Palo Alto, CA, USA) that was positioned 60 cm away from the participants. The screen covered a 36.87 × 28.07° visual field. The spatial resolution of the monitor was 1600 × 1200 pixels, and the vertical refresh rate was 85 Hz. All stimuli were presented on a gray background (32.7 cd/m^2) in grayscale with a luminance range from 0 to 72.5 cd/m^2. All experiments were conducted in a dark room with the display monitor as the main source of illumination. Fig. 1A illustrates the task design consisting of three phases.

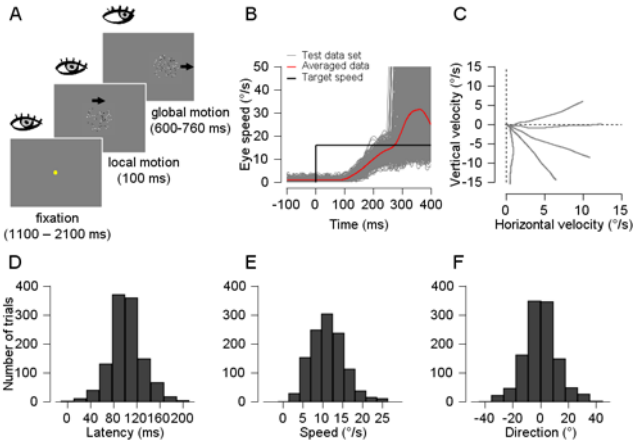

FIGURE 1. The task design. *A*, **Human participants were asked to perform a smooth pursuit eye movement task. The task started when a fixation point (a yellow dot) appeared in the center of the screen. The fixation point remained for a uniformly randomized fixation duration (1100–2100 ms), then disappeared. At the end of the fixation period, a random dot kinematogram appeared at the center of the screen replacing the fixation point; then, all dots in the patch moved in a direction randomly selected from the five directions (0°, 30°, 270°, 300°, or 330°) for 100 ms while the invisible circular patch remained stationary (local motion). Next, the whole patch and dots moved together in the same direction as that of the local motion for 600–760 ms.** *B*, **Representative eye speed traces of participant BSW, from 100 ms before to 400 ms after visual motion onset. Light gray traces show eye speed in individual trials and the red trace shows the mean across trials. The black solid line shows the target speed. Trials that contained any saccadic eye movements in a time-window between −100 and 250 ms from motion onset were manually discarded.** *C*, **Average eye velocity traces of participant BSW for the five pursuit directions in a Cartesian coordinate composed of horizontal and vertical velocity components.** *D*, *E*, *F*, **Histograms of participant SSK's pursuit latency (D), speed (E), and direction (F) from the decomposition analysis. Histograms were made from the analysis of 1143 trials of SSK's pursuit behavior. All three components of smooth pursuit show a substantial amount of trial-by-trial variations.**

1) Fixation period—A small yellow dot (the fixation point, 0.3 × 0.3° in size and 68.2 cd/m^{2}in luminance) was presented at the center of the screen for a random duration between 1100 and 2100 ms (a uniform probability, with 2-ms resolution). Subjects were instructed to focus on the fixation point and maintain the fixation within 2° of the point during the task.

2) Local motion period—Immediately after the extinction of the fixation point, a random dot patch moving at 16 deg/s was presented inside a 4.5°-diameter circular aperture centered on the screen. The patch consisted of 64 black and 64 white dots with 100% contrast, and its mean luminance was the same as that of the background. For the initial 100 ms, the invisible circular aperture was stationary while the dots inside the aperture moved in one of five directions: 0°, 30°, 270°, 300°, or 330°, with 100% coherence. Motion directions were mainly selected from the fourth quadrant because most humans deliver better performance at tracking horizontal and downward motion stimuli than vertical and upward motion stimuli [23]. Subjects were asked to track the moving dot patch smoothly.
3) Global motion period—The aperture and dots inside the aperture moved together for a random duration of 600–790 ms. The direction and speed of the global motion were the same as those of the local motion. Each trial was considered successful if subjects tracked the patch within 5 × 5° of the invisible square window around the moving stimulus smoothly until it stopped and disappeared. Subjects performed 16–19 blocks of 80 trials with a 1000-ms inter-trial delay with 1-minute breaks between blocks. Unfinished trials were discarded. Each participant performed 266.7 trials per condition and total 1333.3 trials on average.

B. DATA ACQUISITION

Eye movements and EEG were recorded with precise synchronization of stimulus presentation. The acquisition of eye position and visual stimulus presentation were controlled through a real-time data-acquisition program (Maestro, https://site.google.com/a/srscicomp.com/maestro/). Eye positions were measured using an infrared eye tracker (EyeLink 1000 Plus, SR Research, Ottawa, ON, Canada) with a sampling rate of 1 kHz. EEG signals were recorded using a 64-channel amplifier (BrainAmp, Brain Products, GmbH, Gilching, Germany) and active electrodes (actiCAP, Brain Products, GmbH) mounted on an elastic cap. The impedance of the electrodes was kept under 25 kΩ during the recordings, and the sampling rate of the EEG data collection was 5 kHz. We used separate computers for controlling visual stimuli and EEG data collection. All behavior-control–related information was transmitted to the EEG data collection computer online through a custom-built hardware interface and digital input and output (I/O) device for later synchronization. We used a custom-built photodiode system to guarantee the precise timing of visual stimuli. All the behavioral and neural data were aligned to the visual stimulus onset timing reported from the photodiode system.

C. EYE-MOVEMENT ANALYSIS

To isolate the initiation of smooth pursuit eye movements, we screened all trials visually and discarded any in which saccadic eye movements happened in the time window of −100 to 250 ms relative to the visual stimulus onset (Fig. 1B). Then, we decomposed the open-loop period of pursuit (approximately the first 100 ms of smooth pursuit from the average pursuit latency; [24], [25]) into speed, direction, and latency components in individual trials using a method described previously [11], [12], [26]. Briefly, we averaged horizontal and vertical velocity traces from all trials in each direction condition and determined the mean pursuit latency by visually inspecting the average velocity traces. We rotated all velocity traces in a polar coordinate so that the rotated velocities would be averaged to 45° for mathematical simplification without changing the data. We obtained the templates for the horizontal and vertical components of eye velocity by averaging eye velocity traces from −20 to 100 ms from the mean latency. Then, we estimated the two best-fitted scaling factors (for the horizontal template and the vertical template) and a latency factor in each trial using the least-square method (NOMAD algorithm; [27]) as follows:

$$E_i^H(\Delta t_i) = E_{template}^H \times a_i^H \tag{1}$$

$$E_i^V(\Delta t_i) = E_{template}^V \times a_i^V \tag{2}$$

where $E_{template}^H$ and $E_{template}^V$ are the velocity templates, E_i^H and E_i^V are horizontal and vertical eye velocity estimates for trial i, and Δt_i is the latency estimate for trial i. a_i^H and a_i^V are the scaling factors of horizontal and vertical eye velocity components in trial i. When average eye velocity traces are rotated to 45°, $E_{template}^H \approx E_{template}^V$. Therefore, speed ($\Delta S_i$) and direction ($\Delta\theta_i$) estimates for trial i were calculated from (3) and (4).

$$\Delta S_i = constant \times \sqrt{\left(a_i^H\right)^2 + \left(a_i^V\right)^2} \tag{3}$$

$$\Delta\theta_i = \tan^{-1}\frac{a_i^V}{a_i^H} \tag{4}$$

We included trials in further analyses only if each estimated function explained more than 50% of data variance to avoid using unreliable estimates of pursuit parameters. To avoid including trials with extreme values of speed, direction, and latency components in the trial-by-trial correlation analysis, we further excluded outliers (i.e., more than two standard deviations from the mean for any of the three components, on average 13% of trials were excluded).

D. PREPROCESSING OF EEG DATA

We preprocessed the recorded EEG data as follows. All preprocessing and analyses were conducted using Matlab (MathWorks, Natick, MA, USA). We used subroutines included in EEGLab [28] and FieldTrip [29] Matlab toolbox packages for signal processing. We down-sampled the EEG data from 5 to 1 kHz and applied a high-pass filter with a 0.1-Hz cutoff frequency for removing slow drifts [30]. We used the Artifact Subspace Reconstruction (ASR) routine [31] to remove noisy channels and re-referenced all data to the mean [32]. We removed line noise (60, 120, and 180 Hz) using the *cleanline* EEGLab plugin [33]. Then, we applied Independent Component Analysis (ICA) [34] to remove signals from the

recorded EEG that were not related to the experiment using EEGLab implementation ''runica'' [28]. Finally, we removed ICs classified as artifacts using the *ADJUST* EEGLab plugin [35]. We band-pass filtered the preprocessed EEG signal into theta (4–8 Hz), alpha (8–13 Hz), beta (13–30 Hz), and gamma (30–50 Hz). We epoched the preprocessed and filtered signals from −400 to 600 ms relative to the visual stimulus onset in each trial. We applied the Hilbert transformation of the filtered data to obtain instantaneous power and phase time courses of each frequency.

To reduce the noise in the time-series data, we obtained the moving average of 20 ms from −200 to 500 ms relative to the onset of visual stimulus at 2-ms intervals. When the event-related potential (ERP) components in the trial-by-trial correlation analysis were used, baseline activity was obtained by averaging EEG activity from 100 to 0 ms before the visual stimulus onset. The baseline activity was subtracted from the time-dependent EEG activity in each trial. In the analysis of the phase and power time courses, we did not subtract the baseline because the on-going oscillatory activity during the fixation duration could contribute to the trial-by-trial variation of smooth pursuit eye movements. (The topographic plots of the power of theta oscillation was an exception. In this case, we converted the power into decibel [dB] using the average baseline theta power from 100 to 0 ms before the visual stimulus onset.) Next, we normalized the data in each channel across trials by converting the EEG activity (ERP and power) into standard scores (z-score). When we analyzed the phase time courses, we took the sine and cosine of the phase and normalized the sine and cosine values individually.

E. LINEAR ESTIMATORS OF SMOOTH PURSUIT VARIATION

We obtained linear estimators of the three components of smooth pursuit eye movements from the z-scored EEG activity pattern using a method that is analogous to that used in a previous study analyzing neural spiking activity [36]. In the previous study, the information in the temporal dynamics of spiking activity that contributed to the variation in oculomotor behavior was considered in the estimators. In this study, we considered the information present in the EEG activity pattern across multiple sensors. This approach is analogous to multiple linear regressions, i.e., estimating regression slopes across the 64 channels that accounted for the latency, speed, or direction variations in the smooth pursuit eye movements. Fig. 2 is a schematic of the data analysis process.

For all trial-by-trial correlation analyses, we used the 'leave one condition out' procedure to prevent overfitting. For example, when we obtained a linear estimator of eye direction on the stimulus motion with a 330° direction (the center direction among the five motion direction conditions), we used trials from the other four directions for estimating the weight matrix. We repeated this procedure for all other directions. Each dataset composed of a $N_{trials} \times N_{channels}$ matrix for each given time point except for the phase time course. In each given time point, we first conducted principal component analysis (PCA) of the EEG activity because EEG activities

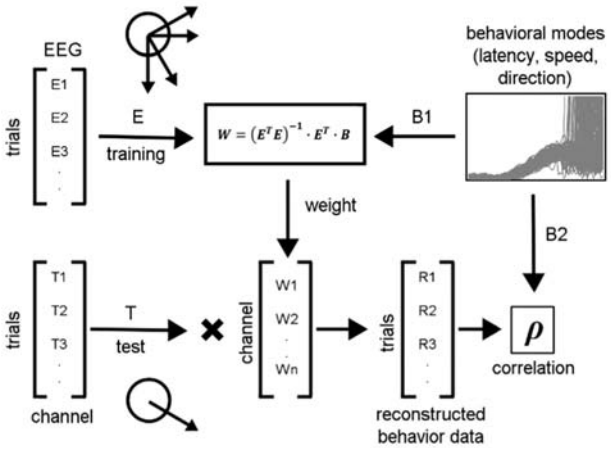

FIGURE 2. The analysis method. EEG data from the central direction (330°) were used as a test set (T) and data from the other directions (0°, 30°, 270°, and 300°) were used as the training set (E). We used this 'leave one condition out' method for all other direction conditions. Weights were calculated from neural data E and behavioral data B1. Linear estimators of behavioral data (R) were obtained by multiplying the neural data from the test set (T) with the estimated weight (W) from the training set. Trial-by-trial correlations (Spearman's rho) between the behavioral data B2 from the test set and the linear estimators R were computed.

are correlated across the channels. All subsequent analyses were conducted on the orthogonalized, principal scores of the EEG data. We obtained a weight matrix ($N_{components} \times 1$) from the principal scores of the z-scored EEG data that could best explain the behavioral variations in a ''least-squared'' sense using (5) and (6).

$$E_1 \cdot W = B_1 \tag{5}$$

$$\hat{W} = \left(E_1^T \cdot E_1\right)^{-1} \cdot E_1^T \cdot B_1 \tag{6}$$

To focus only on the trial-by-trial variations both in behavior and EEG responses, we converted the latency, speed, and direction components of smooth pursuit B_1 ($N_{trials} \times 1$) into standard scores (z-score) by subtracting the means and dividing by the standard deviations across all trials. E_1($N_{trials} \times N_{components}$) contains the principal score of the z-scored EEG data in a given time point. The weight matrix W ($N_{components} \times 1$) was then estimated from (6). Using the estimated weight matrix $\left(\hat{W}\right)$, we obtained the linear estimators of speed, direction, and latency in the test direction by multiplying the principal scores of the z-scored EEG data from the test direction condition with $\hat{W}$.

$$E_2 \cdot \hat{W} = R \tag{7}$$

E_2 ($N_{trials} \times N_{components}$) contains the principal scores of the z-scored EEG data for the test direction and R ($N_{trials} \times 1$) is the linear estimator of the three smooth pursuit components. We computed the trial-by-trial correlations between the linear estimator of eye movement components from the multivariate EEG residual activity and the recorded eye movement components (Spearman's rho). Using this approach, the correlation

coefficient shall always be positive. Therefore, we used bootstrap analysis [37] to convert the correlation coefficient into a standard score to remove any biases when evaluating the significance of the correlations. We shuffled the trials and followed the procedures listed in (1), (2), and (3) for estimating the correlation coefficients. We repeated this shuffle analysis 500 times and generated the "null distribution" of the correlation coefficient. From the distribution of the shuffle analysis, we converted the original correlation coefficient into the z-score. We averaged the z-transformed correlation coefficients across all participants (n = 15) for each time point. A cluster-based permutation test was used to evaluate the significance of correlations [38]. The test was performed with 10000 permutations using a p-value of 0.05 (two-tailed).

In the analysis of phase time course, we implemented a slightly different approach from the method described above because phase angles are not continuous variables. Therefore, we used the sine and cosine of the phases to predict the trial-by-trial variation of smooth pursuit eye movements. Instead of using (5), (6), and (7), we used (8), (9), and (10) to overcome the discontinuous nature of the phase information, utilizing a similar approach implemented in a previous study [39].

$$P_{combined} \cdot W_{combined} = B_1 \tag{8}$$

where $P_{combined} = \left[\sin\theta_1 \ \cos\theta_1 \right]$, $W_{combined} = \begin{bmatrix} W_{sine} \\ W_{cosine} \end{bmatrix}$.

$$\hat{W}_{combined} = \left(P^T_{combined} \cdot P_{combined}\right)^{-1} \cdot P^T_{combined} \cdot B_1 \tag{9}$$

$$P_{test} \cdot \hat{W}_{combined} = \mathrm{R} \tag{10}$$

where $P_{test} = \left[\sin\theta_2 \ \cos\theta_2 \right]$. θ_1 is the instantaneous phase obtained from a Hilbert transformation in the training condition, and θ_2 is the instantaneous phase in the test condition.

In the typical smooth pursuit experiments, pursuit performances in the two outer direction conditions (30° and −90°) were relatively poor with a smaller number of succeeded pursuits. Therefore, we only used the correlations calculated from the three central direction conditions (0°, −30°, and −60°) for further analysis.

F. PRESENTATION OF THE TOPOGRAPHIC PLOT OF THE WEIGHT MATRIX

If the analysis described in Section II E was conducted without applying the PCA on the multivariate EEG activity, the correlations would be the same as those when the PCA was applied on the EEG activity. Therefore, we conducted an identical analysis without applying PCA and calculated the weight matrix to determine the contributions of each sensor to the variation in specific oculomotor behavioral components. Because we took sine and cosine of the phase time course for correlation analysis, we took the geometrical mean of the weight matrices for sine and cosine components following (11).

$$W_{geomean} = \sqrt{W^2_{sine} + W^2_{cosine}} \tag{11}$$

We averaged the combined weight matrix across the 15 participants and divided each value by the standard deviation to consider reliability across participants in the topographical plots.

III. RESULTS

We successfully recorded eye movements and EEG activity simultaneously from 15 human participants while they were engaged in a smooth pursuit eye movement task. We found that phase information in the theta band oscillation (4–8 Hz) could predict the variation in the direction and latency of oculomotor behavior.

A. DECOMPOSITION OF SMOOTH PURSUIT EYE MOVEMENTS

We asked the human participants to perform a visually-guided smooth pursuit eye movement task using a random-dot kinematogram as a visual target for tracking (Fig. 1A). The first 100 ms of smooth pursuit eye movements are known to be guided by visual motion and are free from the influence of movement-related feedback (open-loop pursuit; [24], but see [40] as an exception). We first decomposed these open-loop pursuit responses into three components before we looked for EEG components that predict behavioral variations. The obtained latency, speed, and direction components from the decomposition analysis exhibit a substantial amount of trial-to-trial variation under identical sensory motion conditions (Fig. 1D, 1E, and 1F). For example, eye directions sometimes deviated more than 30° from the mean and overlapped with eye directions from different visual stimulus conditions (Fig. 1F). Therefore, it is important to understand and identify the EEG components that are predictive of the behavioral variation. We developed a novel method (see Section II E) to isolate the EEG activity pattern that is specific for the behavioral component of interest.

B. RESIDUAL MULTIVARIATE ACTIVITY PATTERNS OF EVENT-RELATED POTENTIALS ARE NOT PREDICTIVE OF VARIATION IN BEHAVIORAL MODES

Before we explored the oscillatory components of the EEG activity that were predictive of behavioral variations, we first investigated if the multivariate event-related potentials (ERP, electrophysiological responses to the stimulus) were predictive of pursuit variation. Fig. 3A presents the mean ERP time course (averaged across the 17 posterior channels and 15 participants) and the topographical plots that demonstrate the distribution of ERP activity across the 64 channels. Fig. 3B–D present the resultant z-scored correlation time courses for the three behavioral modes, averaged across participants. Although there were time clusters that were significantly higher than zero for pursuit latency and direction variation, a significant correlation (based on the cluster-based permutation test) was found during the initiation of the smooth pursuit eye movement (122–132 ms from stimulus onset for latency, with average pursuit latency ∼100 ms). A significant correlation was also found after the initiation of

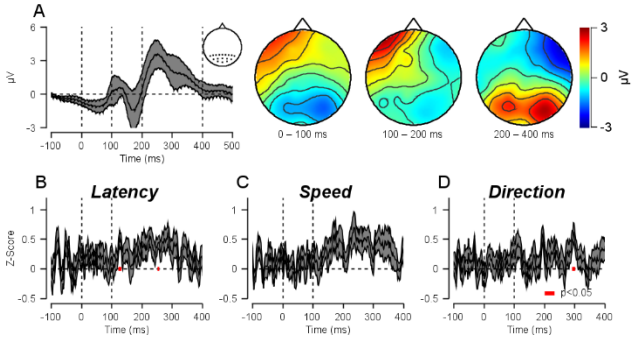

FIGURE 3. **Trial-by-trial correlations between event-related potential (ERP) and behavioral modes of smooth pursuit eye movements.** *A*, **A grand average ERP time course across posterior channels (Pz, P1, P2, P3, P4, P5, P6, P7, P8, POz, PO3, PO4, PO7, PO8, Oz, O1, O2) and across the 15 participants. The gray shaded area shows the standard deviation across participants. An inset figure shows the location of posterior channels. The three topographical plots show the ERP pattern across the 64 channels in the three different time windows (0–100 ms, 100–200 ms, and 200–400 ms).** *B*, **Z-scored trial-by-trial correlations between pursuit latency variation and latency estimate from the multivariate EEG activity.** *C*, **Z-scored trial-by-trial correlations between pursuit speed variation and speed estimate.** *D*, **Z-scored trial-by-trial correlations between pursuit direction variation and direction estimate. Shaded gray areas show the standard error.**

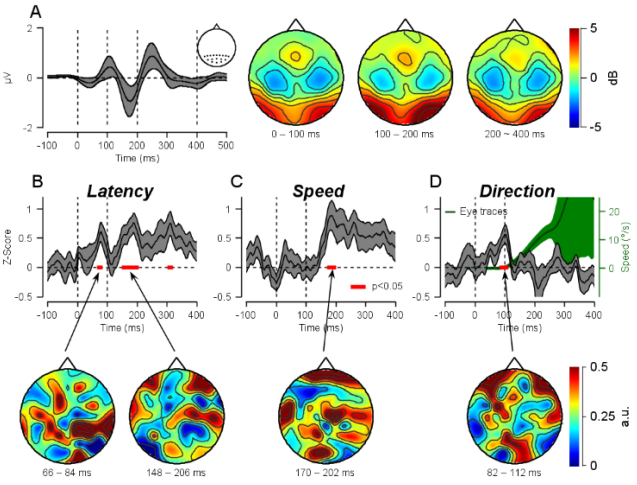

FIGURE 4. **Trial-by-trial correlations between phases of theta oscillation and behavioral modes of smooth pursuit eye movements.** *A*, **A grand average of theta bandpass filtered time course across posterior channels (Pz, P1, P2, P3, P4, P5, P6, P7, P8, POz, PO3, PO4, PO7, PO8, Oz, O1, O2) and the 15 participants. Gray shaded areas show the standard deviation. The three topographical plots show the theta power distributions across the whole channels in the three-time windows (0–100 ms, 100–200 ms, and 200–400 ms). Theta power appears to become stronger after the visual stimlus onset.** *B*, **Z-scored trial-by-trial correlations between pursuit latency variation and the latency estimate from the phases of multivariate theta oscillation.** *C*, **Z-scored trial-by-trial correlations between pursuit speed variation and the speed estimate.** *D*, **Z-scored trial-by-trial correlations between pursuit direction variation and the direction estimate. Shaded gray area shows standard error. Shaded green area shows mean and standard deviation of SSK's eye speed traces. Topographies below each correlation plots showed the average weight matrix across the 15 participants normalized by the standard deviations. The normalized weight matrixes were averaged on each significant time clusters for latency, speed, and direction.**

the pursuit was complete when catch-up saccadic eye movements occurred (252–258 ms for latency, and 292–302 ms for direction). This was significant at $p < 0.01$ for the cluster selection and $p < 0.05$ for the two-sided significance test. Therefore, these correlations were likely induced by smooth pursuit eye movements themselves.

C. PHASES OF THETA OSCILLATION ARE PREDICTIVE OF PURSUIT LATENCY AND DIRECTION VARIATIONS

Next, we investigated if the known oscillatory band activities were predictive of the pursuit variations. We band-pass filtered the EEG activity into four frequency bands (theta 4–8 Hz, alpha 8–13 Hz, beta 13–30 Hz, and gamma 30–50 Hz) and applied the Hilbert transformation to extract instantaneous power and phase time courses. Then, we estimated behavioral modes from multivariate power and phase time courses. Because phase angles have a discontinuity, we took sine and cosine values of the phase angles for estimating the behavioral modes (see Section II E and equations 8–10 for detail). Fig. 4A presents the band-pass filtered EEG in theta frequency (averaged across the 17 posterior channels and 15 participants) and topographical plots that illustrate the distribution of theta power across the 64 channels. Fig. 4B–D presents the z-scored correlation results. We found that the phase of the multivariate theta oscillatory activity predicted variations in pursuit latency and pursuit direction. The typical pursuit latency was ∼100 ms from visual stimulus onset; therefore, the significant correlations that appeared before that time must be predictive of the trial-by-trial variation in smooth pursuit eye movements. Between 66 and 84 ms from visual stimulus onset, the estimated latency mode from the theta phase was significantly correlated with pursuit latency variation (performed using the cluster-based permutation test, using $p < 0.01$ for cluster selection and $p < 0.05$ for the two-sided significance test).

Between 82 and 112 ms from the visual stimulus onset, the estimated direction mode from the multivariate theta phase was significantly correlated with the trial-by-trial variation of pursuit direction. It appears that the multivariate theta phase is not predictive of pursuit speed variation although there is a significant time cluster (performed using the cluster-based permutation test, significance levels as above). The significant time-cluster overlapped with the on-going pursuit behavior, and the earliest time of the significant correlation was approximately 70 ms after the eye started moving (170–202 ms from stimulus onset). Therefore, the significant correlation was likely to be induced by the pursuit eye movement itself. Because we found that the pattern of theta phase variation was indicative of impending smooth pursuit latency and direction, we identified the sensors that were important for the trial-by-trial correlations. We took the geometrical mean of the weight matrix for sine and cosine components of the phase. Interestingly, the contributions of each electrode to the behavioral variations were different, depending on the behavioral mode. For example, in the weight matrix for pursuit latency variation, posterior channels

were more dominant before the eye started moving (66–84 ms from visual stimulus onset). However, both anterior and posterior channels contributed to behavioral direction variation (82–112 ms from visual stimulus onset). Furthermore, the contribution of each channel to the same behavioral mode was different at different times. Anterior channels became more dominant for the latency correlation after the eye started moving (148–206 ms from stimulus onset), which suggests that the underlying neural mechanisms for the trial-by-trial relationship may be different from each other before and after the eye begins to move. These differences suggest that the encodings of behavioral variations in the multivariate EEG theta phase are temporally dynamic [41] and behaviorally mode-specific.

We found that only the multivariate phase information in theta oscillation was predictive of variation in smooth pursuit latency and direction. We applied the identical analysis method on the multivariate phase in alpha, beta, and gamma oscillations, but none passed the cluster-based permutation test with the exception of the relationship between multivariate alpha phase and pursuit latency variation. This correlation appeared far later; thus, it is not predictive of behavioral variations. We could not find any frequency components that were predictive of the oculomotor behavioral modes when we analyzed the power time course (Fig. 5).

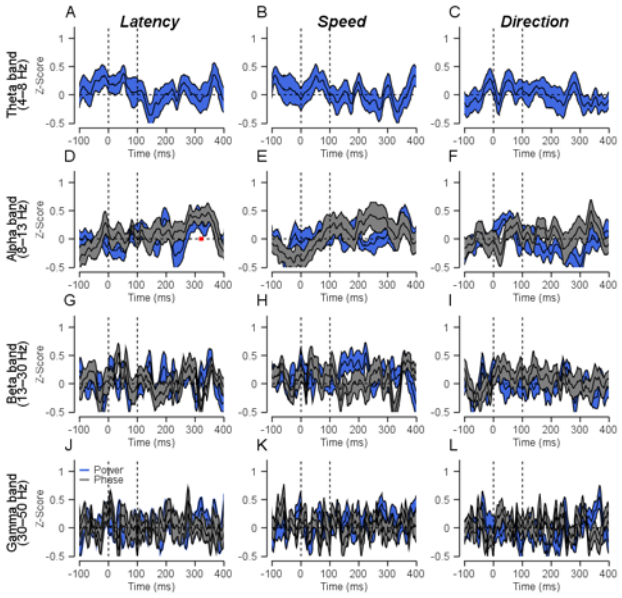

FIGURE 5. Trial-by-trial correlations between multivariate EEG activities in different frequency bands and smooth pursuit latency, speed, and direction. *A–C*, Trial-by-trial correlation between power of multivariate theta oscillation and smooth pursuit latency (A), speed (B), and direction (C) variation. *D–F*, Trial-by-trial correlation between powers and phases of multivariate alpha oscillation and smooth pursuit latency (D), speed (E), and direction (F) variation. *G–I*, Trial-by-trial correlation between powers and phases of multivariate beta oscillation and smooth pursuit latency (G), speed (H), and direction (I) variation. *J–L*, Trial-by-trial correlation between powers and phases of multivariate gamma oscillation and smooth pursuit latency (J), speed (K), and direction (L) variation. Gray color showed the z-scored phase correlation and blue color showed the z-scored power correlations. Gray and blue shaded areas showed the standard errors.

IV. DISCUSSION

Our study demonstrates that the multivariate theta phase is predictive of the variation in smooth pursuit latency and direction. We devised a method that enabled us to isolate the EEG activity components that were specific to the variation of sensory-motor behavioral mode (smooth pursuit latency, speed, and direction), and successfully identified the oscillatory components that are meaningful for controlling pursuit latency and direction variations.

Recent studies have employed the multivariate analysis method on EEG data to understand how EEG activity represents various stimulus properties. Using the inverted encoding model [42] and others, several studies have shown how stimulus orientation information is maintained in working memory [43]–[47] and modeled the effect of attention [48] on the oriented visual stimulus. A recent study represented visual and pursuit motion information in multivariate EEG activity during smooth pursuit eye movements [22]. These studies all used multivariate pattern analysis to extract the specific stimulus information of interest (for example, stimulus orientation), which is a step forward in EEG research and applications. Nonetheless, these studies only focus on the stimulus information that is represented in the EEG activity pattern.

We show that there is often a substantial amount of behavioral variation, even if the stimulus condition and intended movements are the same. Although behavioral response measurements in the smooth pursuit eye movement task are supposed to be less noisy than other sensory-motor behaviors (because it is a simple and reactive one), the measured behavioral variations to the same stimulus sometimes exceed behavioral differences induced by different visual motions, as found in this study. Therefore, it is important to isolate the relevant EEG activity pattern for a specific behavioral variation. The neural marker of behavioral variation can contribute to improving the signal to noise ratio of EEG activity decoding, which can be used in the development of a precise brain-computer interface system for rehabilitation applications [20]. In this study, we took advantage of the multivariate pattern analysis of EEG for isolating the neural components that are specific to the variation of smooth pursuit latency, speed, and direction. In this novel analysis, we were careful to obtain robust and reliable correlations. First, we used the 'leave one condition out' method to prevent overfitting in the estimation of the pursuit modes (latency, speed, and direction) from EEG activity. Second, we used a permutation approach to avoid any errors or biases in interpreting the significance of the correlations.

Even if we reliably estimated and found the neural marker for the behavioral variations, some remaining questions and issues need to be addressed in the future. First, our method is ignorant of dynamical interactions across channels and the role of these dynamics on the behavioral variations. To understand the underlying neural dynamics and connectivities

across brain areas, we should investigate the temporal dynamics of multichannel EEG activities themselves using multivariate autoregressive models, for example, state-space models [49], [50], Granger causality analysis [51], [52], or dynamical causal modeling [53], [54]. Second, although we found the neural correlates, we still do not know how this component is coupled with behavioral variations. It is intriguing that only the phases of the multivariate theta oscillation were predictive of the impeding motor behavior. Previous studies have shown that the phase of theta oscillation has important roles in navigation [55], attentional sampling [56]–[58], and perception [59], [60]. Some recent studies demonstrated that hippocampal augmentation of theta oscillation is associated with movement onset [61], [62]. These results suggest that theta oscillation might have an important role in motor-related cognitive functions. Another study showed that theta oscillations are phase-locked to the onset of the movement, and in this case, the phases were predictive of perception [39]. Therefore, in our study, the theta phase might be related to the perception of the pursuit targets that are tightly coupled to the following eye movements.

The other notable aspect is that we only found significant, predictive correlations for pursuit latency and direction. The correlations for speed appeared after the eye started moving, thus the correlation might have been induced by behavior. We speculate and note that the predictive role of the multivariate theta phase could be because of our task design. In this study, participants had to predict the timing and direction of the incoming pursuit target because they did not know when the target stimulus would appear, and the motion direction was randomly selected. We used the same speed of 16 deg/s across the trials in a given day, so there was no uncertainty regarding the speed of the pursuit target. If the variation of spatially distributed theta phase has a key role in prediction, the absence of the correlation in pursuit speed variation can be explained by this 'predictive coding' hypothesis [63]. Consistent with this scheme, previous studies revealed the role of theta oscillation in predictive control in learning [64]–[66]. If that is the case, the trial-by-trial correlation with the theta phase will dynamically change depending on whether the participants need a prediction of the incoming sensory stimulus feature or not. If the speed of the pursuit target is randomized, the theta phase will become predictive for pursuit speed variation. This hypothesis remains to be tested in future studies.

V. CONCLUSION

Our study indicates that trial-by-trial variation in oculomotor behavioral modes can be predicted by the multivariate phase of theta oscillation. Given that there is a substantial amount of trial-by-trial variation in behavioral responses and that the neural components specific to the behavioral errors are distinct, our study contributes toward a comprehensive understanding of the underlying neural mechanisms for smooth pursuit eye movements in humans. The analysis method and approach can be broadly applied to other sensory-motor behaviors. An understanding of neural sources for behavioral variations in human EEG recordings will facilitate the development of a precise brain-computer interface system.

VI. ACKNOWLEDGMENT

The authors would like to thank Jeongjun Park, Joonsik Moon, Kyoungmin Kim, and Hyomin Yu for assisting with data collection. They also would like to thank Dr. Min-Suk Kang and Dr. Seong-Gi Kim for constructive suggestions for the earlier versions of the manuscript.

REFERENCES

[1] E. Todorov and M. I. Jordan, "Optimal feedback control as a theory of motor coordination," *Nature Neurosci.*, vol. 5, no. 11, pp. 1226–1235, Nov. 2002.

[2] M. N. Shadlen and W. T. Newsome, "Noise, neural codes and cortical organization," *Current Opinion Neurobiol.*, vol. 4, no. 4, pp. 569–579, Aug. 1994.

[3] A. Pouget, A. Pouget, P. Dayan, P. Dayan, R. Zemel, and R. Zemel, "Information processing with population codes," *Nature Rev. Neurosci.*, vol. 1, no. 2, pp. 125–132, Nov. 2000.

[4] B. B. Averbeck, P. E. Latham, and A. Pouget, "Neural correlations, population coding and computation," New York, NY, USA, vol. 7, May 2006.

[5] R. Desimone and L. G. Ungerleider, "Multiple visual areas in the caudal superior temporal sulcus of the macaque," *J. Comparative Neurol.*, vol. 248, no. 2, pp. 164–189, Jun. 1986.

[6] N. J. Priebe, C. R. Cassanello, and S. G. Lisberger, "The neural representation of speed in macaque area MT/V5," *J. Neurosci.*, vol. 23, no. 13, pp. 5650–5661, Jul. 2003.

[7] J. Ditterich, M. E. Mazurek, and M. N. Shadlen, "Microstimulation of visual cortex affects the speed of perceptual decisions," *Nature Neurosci.*, vol. 6, no. 8, pp. 891–898, Aug. 2003.

[8] J. H. Maunsell and D. C. Van Essen, "Functional properties of neurons in middle temporal visual area of the macaque monkey. I. selectivity for stimulus direction, speed, and orientation," *J. Neurophysiol.*, vol. 49, no. 5, pp. 1127–1147, May 1983.

[9] J. M. Groh, R. T. Born, and W. T. Newsome, "How is a sensory map read out? Effects of microstimulation in visual area MT on saccades and smooth pursuit eye movements," *J. Neurosci.*, vol. 17, no. 11, pp. 4312–4330, Jun. 1997.

[10] S. S. Hohl, K. S. Chaisanguanthum, and S. G. Lisberger, "Sensory population decoding for visually guided movements," *Neuron*, vol. 79, no. 1, pp. 167–179, Jul. 2013.

[11] J. Lee and S. G. Lisberger, "Gamma synchrony predicts neuron-neuron correlations and correlations with motor behavior in extrastriate visual area MT," *J. Neurosci.*, vol. 33, no. 50, pp. 19677–19688, Dec. 2013.

[12] J. Lee, M. Joshua, J. F. Medina, and S. G. Lisberger, "Signal, noise, and variation in neural and sensory-motor latency," *Neuron*, vol. 90, no. 1, pp. 165–176, Apr. 2016.

[13] M. Tanaka and S. G. Lisberger, "Role of arcuate frontal cortex of monkeys in smooth pursuit eye Movements. I. basic response properties to retinal image motion and position," *J. Neurophysiol.*, vol. 87, no. 6, pp. 2684–2699, Jun. 2002.

[14] M. Tanaka and S. G. Lisberger, "Regulation of the gain of visually guided smooth-pursuit eye movements by frontal cortex," *Nature*, vol. 409, no. 6817, pp. 191–194, Jan. 2001.

[15] J. Lee, T. R. Darlington, and S. G. Lisberger, "The neural basis for response latency in a sensory-motor behavior," *Cerebral Cortex*, Dec. 2019, Art. no. bhz294.

[16] J. F. Medina and S. G. Lisberger, "Variation, signal, and noise in cerebellar sensory-motor processing for smooth-pursuit eye movements," *J. Neurosci.*, vol. 27, no. 25, pp. 6832–6842, Jun. 2007.

[17] M. Joshua and S. G. Lisberger, "A framework for using signal, noise, and variation to determine whether the brain controls movement synergies or single muscles," *J. Neurophysiol.*, vol. 111, no. 4, pp. 733–745, Feb. 2014.

[18] L. C. Osborne, S. G. Lisberger, and W. Bialek, "A sensory source for motor variation," *Nature*, vol. 437, no. 7057, pp. 412–416, Sep. 2005.

[19] D. J. McFarland and J. R. Wolpaw, "EEG-based brain-computer interfaces," *Current Opinion Biomed. Eng.*, vol. 4, pp. 194–200, Dec. 2017.

[20] I. Lazarou, S. Nikolopoulos, P. C. Petrantonakis, I. Kompatsiaris, and M. Tsolaki, "EEG-based Brain–Computer interfaces for communication and rehabilitation of people with motor impairment: A novel approach of the 21st century," *Frontiers Hum. Neurosci.*, vol. 12, pp. 1–18, Jan. 2018.
[21] L. Waschke, S. Tune, and J. Obleser, "Local cortical desynchronization and pupil-linked arousal differentially shape brain states for optimal sensory performance," *Elife*, vol. 8, Dec. 2019, Art. no. e51501.
[22] W. Jeong, S. Kim, Y.-J. Kim, and J. Lee, "Motion direction representation in multivariate electroencephalography activity for smooth pursuit eye movements," *NeuroImage*, vol. 202, Nov. 2019, Art. no. 116160.
[23] K. L. Grasse and S. G. Lisberger, "Analysis of a naturally occurring asymmetry in vertical smooth pursuit eye movements in a monkey," *J. Neurophysiol.*, vol. 67, no. 1, pp. 164–179, Jan. 1992.
[24] S. Lisberger and L. Westbrook, "Properties of visual inputs that initiate horizontal smooth pursuit eye movements in monkeys," *J. Neurosci.*, vol. 5, no. 6, pp. 1662–1673, Jun. 1985.
[25] L. Tychsen and S. G. Lisberger, "Visual motion processing for the initiation of smooth-pursuit eye movements in humans," *J. Neurophysiol.*, vol. 56, no. 4, pp. 953–968, Oct. 1986.
[26] S. Kim, J. Park, and J. Lee, "Effect of prior direction expectation on the accuracy and precision of smooth pursuit eye movements," *Frontiers Syst. Neurosci.*, vol. 13, pp. 1–12, Nov. 2019.
[27] S. Le Digabel, "Algorithm 909: NOMAD: Nonlinear optimization with the MADS algorithm," *ACM Trans. Math. Softw.*, vol. 37, no. 4, pp. 1–15, Feb. 2011.
[28] A. Delorme and S. Makeig, "EEGLAB: An open source toolbox for analysis of single-trial EEG dynamics including independent component analysis," *J. Neurosci. Methods*, vol. 134, no. 1, pp. 9–21, Mar. 2004.
[29] R. Oostenveld, P. Fries, E. Maris, and J.-M. Schoffelen, "FieldTrip: Open source software for advanced analysis of MEG, EEG, and invasive electrophysiological data," *Comput. Intell. Neurosci.*, vol. 2011, pp. 1–9, 2011.
[30] I. Winkler, S. Debener, K.-R. Muller, and M. Tangermann, "On the influence of high-pass filtering on ICA-based artifact reduction in EEG-ERP," in *Proc. 37th Annu. Int. Conf. IEEE Eng. Med. Biol. Soc. (EMBC)*, Aug. 2015, pp. 4101–4105.
[31] T. R. Mullen, C. A. E. Kothe, Y. M. Chi, A. Ojeda, T. Kerth, S. Makeig, T.-P. Jung, and G. Cauwenberghs, "Real-time neuroimaging and cognitive monitoring using wearable dry EEG," *IEEE Trans. Biomed. Eng.*, vol. 62, no. 11, pp. 2553–2567, Nov. 2015.
[32] N. Bigdely-Shamlo, T. Mullen, C. Kothe, K.-M. Su, and K. A. Robbins, "The PREP pipeline: Standardized preprocessing for large-scale EEG analysis," *Frontiers Neuroinform.*, vol. 9, p. 16, Jun. 2015.
[33] T. Mullen, "CleanLine EEGLAB Plugin," Neuroimaging Inform. Tools Resour. Clearinghouse (NITRC), San Diego, CA, USA, 2012.
[34] S. Makeig, T.-P. Jung, A. J. Bell, and T. J. Sejnowski, "Independent component analysis of electroencephalographic data," in *Proc. Adv. Neural Inf. Process. Syst.*, no. 3, 1996, pp. 145–151.
[35] A. Mognon, J. Jovicich, L. Bruzzone, and M. Buiatti, "ADJUST: An automatic EEG artifact detector based on the joint use of spatial and temporal features," *Psychophysiology*, vol. 48, no. 2, pp. 229–240, Feb. 2011.
[36] K. S. Chaisanguanthum, M. Joshua, J. F. Medina, W. Bialek, and S. G. Lisberger, "The neural code for motor control in the cerebellum and oculomotor brainstem," *eNeuro*, vol. 1, no. 1, Nov. 2014, Art. no. e0004-14.2014.
[37] B. Efron, "Bootstrap methods: Another look at the jackknife," *Ann. Stat.*, vol. 7, no. 1, pp. 1–26, 1979.
[38] E. Maris and R. Oostenveld, "Nonparametric statistical testing of EEG- and MEG-data," *J. Neurosci. Methods*, vol. 164, no. 1, pp. 177–190, Aug. 2007.
[39] A. Tomassini, L. Ambrogioni, W. P. Medendorp, and E. Maris, "Theta oscillations locked to intended actions rhythmically modulate perception," *eLife*, vol. 6, pp. 1–18, Jul. 2017.
[40] A. Buonocore, J. Skinner, and Z. M. Hafed, "Eye position error influence over 'open-loop' smooth pursuit initiation," *J. Neurosci.*, vol. 39, no. 14, pp. 2709–2721, Apr. 2019.
[41] J.-R. King and S. Dehaene, "Characterizing the dynamics of mental representations: The temporal generalization method," *Trends Cognit. Sci.*, vol. 18, no. 4, pp. 203–210, Apr. 2014.
[42] G. J. Brouwer and D. J. Heeger, "Decoding and reconstructing color from responses in human visual cortex," *J. Neurosci.*, vol. 29, no. 44, pp. 13992–14003, Nov. 2009.
[43] M. J. Wolff, J. Ding, N. E. Myers, and M. G. Stokes, "Revealing hidden states in visual working memory using electroencephalography," *Frontiers Syst. Neurosci.*, vol. 9, pp. 1–12, Sep. 2015.
[44] M. J. Wolff, J. Jochim, E. G. Akyürek, and M. G. Stokes, "Dynamic hidden states underlying working-memory-guided behavior," *Nature Neurosci.*, vol. 20, no. 6, pp. 864–871, Jun. 2017.
[45] D. E. Anderson, J. T. Serences, E. K. Vogel, and E. Awh, "Induced alpha rhythms track the content and quality of visual working memory representations with high temporal precision," *J. Neurosci.*, vol. 34, no. 22, pp. 7587–7599, May 2014.
[46] B.-I. Oh, Y.-J. Kim, and M.-S. Kang, "Ensemble representations reveal distinct neural coding of visual working memory," *Nature Commun.*, vol. 10, no. 1, p. 5665, Dec. 2019.
[47] N. E. Myers, G. Rohenkohl, V. Wyart, M. W. Woolrich, A. C. Nobre, and M. G. Stokes, "Testing sensory evidence against mnemonic templates," *eLife*, vol. 4, pp. 1–25, Dec. 2015.
[48] J. O. Garcia, R. Srinivasan, and J. T. Serences, "Near-Real-Time feature-selective modulations in human cortex," *Current Biol.*, vol. 23, no. 6, pp. 515–522, Mar. 2013.
[49] B. L. P. Cheung, B. A. Riedner, G. Tononi, and B. Van Veen, "Estimation of cortical connectivity from EEG using state-space models," *IEEE Trans. Biomed. Eng.*, vol. 57, no. 9, pp. 2122–2134, Sep. 2010.
[50] T. Tu, J. Paisley, S. Haufe, and P. Sajda, "A state-space model for inferring effective connectivity of latent neural dynamics from simultaneous EEG/fMRI," in *Proc. Adv. Neural Inf. Process. Syst.*, 2019, pp. 1–10.
[51] K. Friston, R. Moran, and A. K. Seth, "Analysing connectivity with Granger causality and dynamic causal modelling," *Current Opinion Neurobiol.*, vol. 23, no. 2, pp. 172–178, Apr. 2013.
[52] A. B. Barrett, M. Murphy, M.-A. Bruno, Q. Noirhomme, M. Boly, S. Laureys, and A. K. Seth, "Granger causality analysis of steady-state electroencephalographic signals during propofol-induced anaesthesia," *PLoS ONE*, vol. 7, no. 1, Jan. 2012, Art. no. e29072.
[53] K. J. Friston, L. Harrison, and W. Penny, "Dynamic causal modelling," *NeuroImage*, vol. 19, no. 4, pp. 1273–1302, Aug. 2003.
[54] S. J. Kiebel, M. I. Garrido, R. Moran, C.-C. Chen, and K. J. Friston, "Dynamic causal modeling for EEG and MEG," *Hum. Brain Mapping*, vol. 30, no. 6, pp. 1866–1876, Jun. 2009.
[55] L. Kunz, L. Wang, D. Lachner-Piza, H. Zhang, A. Brandt, M. Dümpelmann, P. C. Reinacher, V. A. Coenen, D. Chen, W.-X. Wang, W. Zhou, S. Liang, P. Grewe, C. G. Bien, A. Bierbrauer, T. Navarro Schröder, A. Schulze-Bonhage, and N. Axmacher, "Hippocampal theta phases organize the reactivation of large-scale electrophysiological representations during goal-directed navigation," *Sci. Adv.*, vol. 5, no. 7, Jul. 2019, Art. no. eaav8192.
[56] N. A. Busch and R. VanRullen, "Spontaneous EEG oscillations reveal periodic sampling of visual attention," *Proc. Nat. Acad. Sci. USA*, vol. 107, no. 37, pp. 16048–16053, Sep. 2010.
[57] I. C. Fiebelkorn, Y. B. Saalmann, and S. Kastner, "Rhythmic sampling within and between objects despite sustained attention at a cued location," *Current Biol.*, vol. 23, no. 24, pp. 2553–2558, Dec. 2013.
[58] A. Landau,"Distributed attention is implemented through theta-rhythmic gamma modulation," *J. Vis.*, vol. 15, no. 12, p. 1398, Sep. 2015.
[59] R. VanRullen, "Perceptual cycles," *J. Vis.*, vol. 15, no. 12, p. 1401, Sep. 2015.
[60] S. Hanslmayr, G. Volberg, M. Wimber, S. S. Dalal, and M. W. Greenlee, "Prestimulus oscillatory phase at 7 hz gates cortical information flow and visual perception," *Current Biol.*, vol. 23, no. 22, pp. 2273–2278, Nov. 2013.
[61] D. Bush, J. A. Bisby, C. M. Bird, S. Gollwitzer, R. Rodionov, B. Diehl, A. W. McEvoy, M. C. Walker, and N. Burgess, "Human hippocampal theta power indicates movement onset and distance travelled," *Proc. Nat. Acad. Sci. USA*, vol. 114, no. 46, pp. 12297–12302, Nov. 2017.
[62] R. Kaplan, C. F. Doeller, G. R. Barnes, V. Litvak, E. Düzel, P. A. Bandettini, and N. Burgess, "Movement-related theta rhythm in humans: Coordinating self-directed hippocampal learning," *PLoS Biol.*, vol. 10, no. 2, Feb. 2012, Art. no. e1001267.
[63] K. Friston, J. Kilner, and L. Harrison, "A free energy principle for the brain," *J. Physiol.-Paris*, vol. 100, nos. 1–3, pp. 70–87, 2006.
[64] J. F. Cavanagh, C. M. Figueroa, M. X. Cohen, and M. J. Frank, "Frontal theta reflects uncertainty and unexpectedness during exploration and exploitation," *Cerebral Cortex*, vol. 22, no. 11, pp. 2575–2586, Nov. 2012.
[65] J. F. Cavanagh, M. J. Frank, T. J. Klein, and J. J. B. Allen, "Frontal theta links prediction errors to behavioral adaptation in reinforcement learning," *NeuroImage*, vol. 49, no. 4, pp. 3198–3209, Feb. 2010.
[66] J. Crivelli-Decker, L.-T. Hsieh, A. Clarke, and C. Ranganath, "Theta oscillations promote temporal sequence learning," *Neurobiol. Learn. Memory*, vol. 153, pp. 92–103, Sep. 2018.

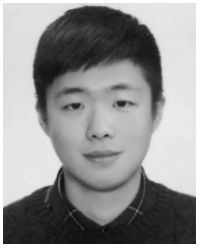

WOOJAE JEONG received the B.S. degree from the Department of Electronic and Electrical Engineering, Sungkyunkwan University, Suwon, South Korea, in 2017, and the M.S. degree from the Department of Biomedical Engineering, Sungkyunkwan University, in 2019. He is currently a Researcher with the Center for Neuroscience Imaging Research, Institute for Basic Science, Suwon. His research interests include computational neuroscience, brain–machine interfaces, and signal processing.

SEOLMIN KIM received the B.S. and M.S. degrees from the Department of Biological Sciences, Sungkyunkwan University, Suwon, South Korea, in 2011 and 2013, respectively, where she is currently pursuing the Ph.D. degree with the Department of Biomedical Engineering. Her research interests include neural networks and neural mechanisms of attention.

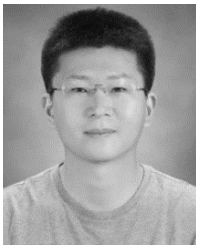

YEE-JOON KIM received the B.S. and M.S. degrees in physics from Seoul National University, Seoul, South Korea, in 1998 and 2000, respectively, and the Ph.D. degree in psychology from Northwestern University, Evanston, IL, USA, in 2008. He was a Postdoctoral Researcher with New York University, New York, NY, USA, from 2008 to 2010, and the Smith-Kettlewell Eye Research Institute, San Francisco, CA, USA, from 2010 to 2014. He is currently a Principal Investigator with the Center for Cognition and Sociality, Institute for Basic Science, Daejeon, South Korea. His research interests include neural basis of sensation, perception, and awareness.

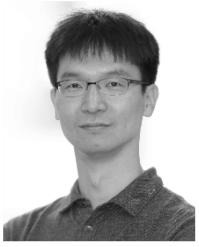

JOONYEOL LEE (Member, IEEE) received the M.A. degree in psychology from Seoul National University, Seoul, South Korea, in 2002, and the Ph.D. degree in neuroscience from the Baylor College of Medicine, Houston, TX, USA, in 2008. He was a Postdoctoral Researcher with the Howard Hughes Medical Institute, Chevy Chase, MD, USA, from 2009 to 2015. He was also a Research Associate with the University of California at San Francisco, San Francisco, CA, USA, from 2009 to 2012, and Duke University, Durham, NC, USA, from 2012 to 2015. He is currently an Assistant Professor with the Department of Biomedical Engineering, Sungkyunkwan University, Suwon, South Korea. His research interests include neural mechanisms of sensory-motor transformation, neural implementation of Bayesian inference, brain–computer interfaces, and statistical signal processing.